

High-resolution Sensing Sheet for Structural-health Monitoring via Scalable Interfacing of Flexible Electronics with High-performance ICs

Yingzhe Hu, Warren Rieutort-Louis, Josue Sanz-Robinson, Katherine Song,
James C. Sturm, Sigurd Wagner, Naveen Verma
Princeton University, Princeton, NJ

Abstract

Early-stage damage detection for buildings and bridges requires continuously sensing and assessing strain over large surfaces, yet with centimeter-scale resolution. To achieve this, we present a sensing sheet that combines high-performance ICs with flexible electronics, allowing bonding to such surfaces. The flexible electronics integrates thin-film strain gauges and amorphous-silicon control circuits, patterned on a polyimide sheet that can potentially span large areas. Non-contact links couple digital and analog signals to the ICs, allowing many ICs to be introduced via low-cost sheet lamination for energy-efficient readout and computation over a large number of sensors. Communication between distributed ICs is achieved by transceivers that exploit low-loss interconnects patterned on the polyimide sheet; the transceivers self-calibrate to the interconnect impedance to maximize transmit SNR. The system achieves multi-channel strain readout with sensitivity of $18\mu\text{Strain}_{\text{RMS}}$ at an energy per measurement of 270nJ, while the communication energy is 12.8pJ/3.3pJ per bit (Tx/Rx) over 7.5m.

System Approach

Large-area electronics (LAE) is based on processing thin films at low temperatures. This allows a broad range of materials to be used for creating diverse transducers on large ($>10\text{m}^2$), conformal substrates [1,2]. Although, thin-film transistors (TFTs) are also possible (using organics, amorphous-silicon (a-Si:H), metal-oxides, etc.), these have orders of magnitude lower performance and energy efficiency than crystalline silicon ICs. Fig. 1 shows the proposed *sensor-network-on-foil* concept, aimed at achieving scalable sensing *and* high-performance computation, by extensively combining ICs with a flexible LAE sheet. The IC-to-LAE interfaces pose the primary limitation to system scalability. To overcome this, non-contact coupling is employed. Inductive and capacitive antennas are patterned on both the LAE sheet and on the flex-tape packaging of the ICs. We achieve assembly via sheet lamination, with typical adhesive thickness $<100\mu\text{m}$; this enables proximity coupling with low energy.

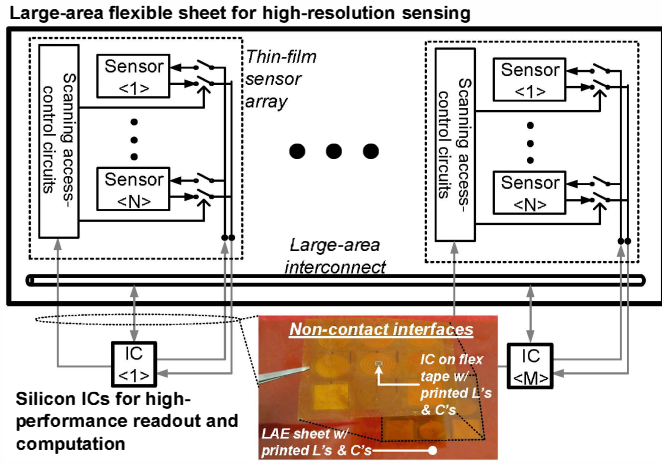


Fig. 1. Scalable sensor-network-on-foil system concept.

To substantially reduce the total number of signals required from the ICs, the LAE sheet integrates TFT-based control and access circuits that enable sequential access to individual strain

sensors in the array. The ICs integrate instrumentation and signal-generation circuits for access control, AC biasing, and readout over the sensor array. For communication over the distributed sheet, the ICs use transceivers that exploit low-loss, large-area interconnects. The interconnect impedance substantially affects the energy and SNR of communication; the transmitters thus self-calibrate to the resonant point of the interconnect, which is difficult to otherwise predict in a large-scale sheet.

Thin-film LAE Circuits for Sensor-array Control

Fig. 2 shows the fully passive LAE circuits. Just four signals are required from the IC for both power and control, to sequentially access the individual sensors. We fabricate the circuits using a-Si:H [3] (this is currently the most stable LAE semiconductor). The mobility ($\sim 1\text{cm}^2/\text{Vs}$) and unipolar (n-channel) nature is similar to other LAE technologies (e.g., organics, oxides, etc.), making the topologies transferrable.

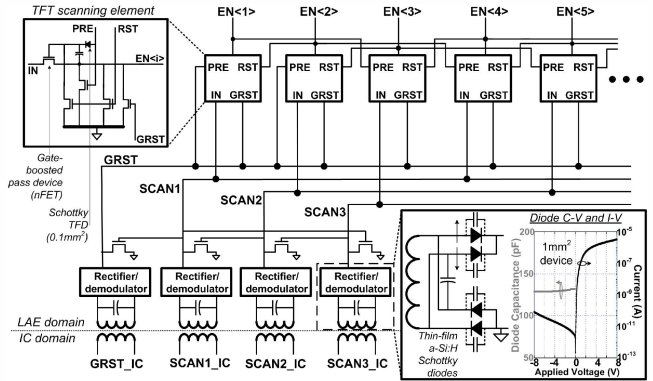


Fig. 2. Thin-film LAE circuits for access control of multiple sensors.

While the IC operates at 1.2V, the LAE circuits need over 6V for reasonable performance. The inductive interfaces, which require AC-modulated IC control signals, can provide voltage step-up. This, however, increases the power of the IC power amplifiers and/or requires high-Q inductors. Though thin-film diodes (TFDs) have been reported [4], we develop a-Si:H Schottky TFDs for low-voltage drop and good rectification characteristics, to demodulate the IC signals (measured I-V and capacitance curves are shown in Fig. 2). In the full-wave rectifier configuration shown, the AC current through the TFD capacitances is cancelled since the inputs oscillate in counter phase. This enables rectification of high frequencies. The interfaces use a frequency of 2MHz, yielding a quality factor of 126 for 2cm planar inductors.

The scanning elements form a chain that uses 3-phase control, with SCAN1-3 asserted in round-robin manner. The Nth scanning element receives a precharge signal (PRE) from the N-2 element and a reset signal (RST) from the N+1 element to control an nFET pass device (the first two elements are precharged by GRST). The sensor enable signals (EN<i>) are thus asserted one-at-a-time down the chain. Since only nFETs can readily be created using a-Si:H, capacitive bootstrapping is used on the pass device to preserve the 6V logic level throughout the circuit (this is achieved using the low-voltage-drop Schottky TFDs).

Instrumentation Circuits for Sensor Readout

Fig. 3 shows the multi-sensor readout circuit. Thin-film resistive strain gauges, calibrated for aluminum beams and having

standardized resistance of $1k\Omega$, are used. Large access TFTs, which are controlled by the scanning circuits, gate the AC biasing signal ($V_{L2} = 0.6V_{AMP}$), which is provided by the IC over an inductive interface. The IC's PA operates in class-C mode, rather than class-D, since the power required is relatively low for practical values of the frequency (5MHz) and the patterned inductors ($3.5\mu H$) (higher frequencies are limited by the parasitics of the access TFTs, and larger inductors are limited by physical size). The PA's duty cycle is optimized to 20%, yielding a measured efficiency of 82%. The AC-modulated sensor signal is then acquired through a capacitive interface (this results in reduced loading on the sensor bridge). Demodulation and readout is then performed via a synchronous G_M -C integrator. Synchronization requires that the PA have proper phase, which is thus achieved via a tunable delay line. The G_M stage demodulates the sensor signal for integration by a low-power op-amp. Demodulation at the G_M stage output mitigates $1/f$ noise and helps reject error signals of orthogonal phase that originate from admittance mismatches in the branches of the sensor bridge.

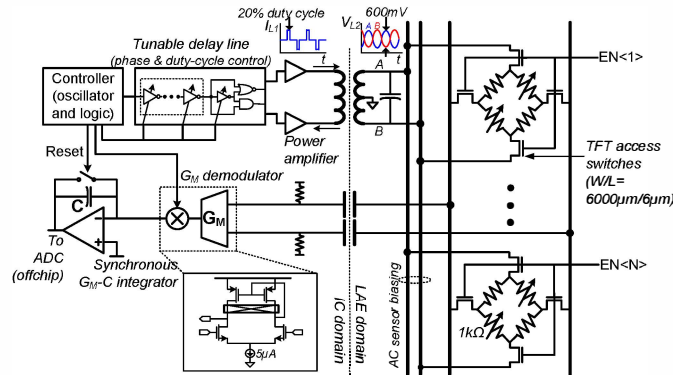


Fig. 3. Multi-sensor readout circuit for thin-film resistive strain-gauge bridges.

Transceiver for Macro-range Communication

Fig. 4 shows the transceiver for communication over distributed ICs. Previous efforts to exploit large-area interconnects have used pulsed signals and have been limited by the interconnect impedance [5]. For strong coupling over the non-contact links, we use AC signaling with on-off keying. The severe and unpredictable interconnect impedance is overcome using an 8-bit digitally-controlled oscillator (DCO) to self-tune the transmitter carrier frequency to the resonant point of the full interconnect network. The local receiver self-senses the transmitted signal, allowing a DCO code to be selected via a gradient descent algorithm to result in the largest amplitude (a measured DCO sweep is shown). To recover digital data, the receiver uses a preamplifier and peak-detector, each biased with $3\mu A$. Synchronization and multiple access between transceivers can be achieved by digital-baseband processing (not included on chip).

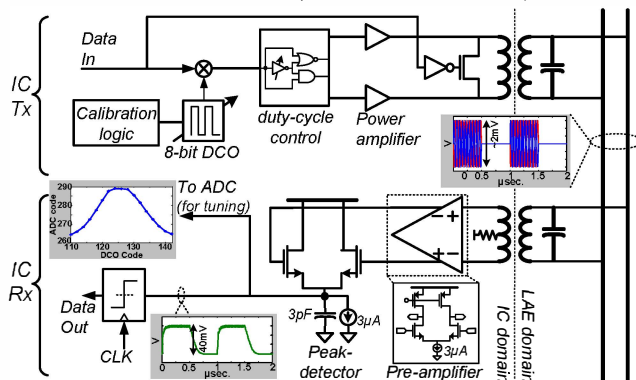


Fig. 4. Transceiver circuits for communication over distributed ICs using large-area interconnects.

Measurement Results

We fabricated the LAE circuits on $50\mu m$ polyimide foil, and the ICs are fabricated in 130nm CMOS from IBM. Fig. 5 shows prototype photographs. Fig. 6 gives measured waveforms, showing the LAE rectifier and scanning circuits generating digital enable signals ($>6V$) from 1.2V, AC-modulated IC control signals. The enable pulses can switch at a rate of 500Hz, limited by the load capacitance of the TFT sensor-access switches (Fig. 3).

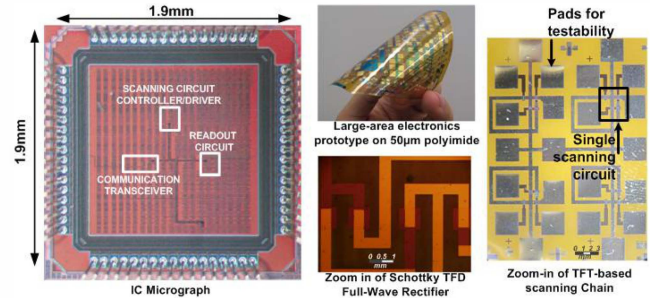


Fig. 5. Micrographs of the 130nm CMOS IC and large-area electronics components we fabricated on $50\mu m$ -thick polyimide.

Fig. 7 summarizes the measurements. Readout-circuit outputs (digitized by an ADC) are shown for sensing applied to a $30cm \times 180cm$ cantilever beam (outputs are correlated with readings from a commercial strain reader, Vishay 3800). The total readout noise is $18\mu Strain_{RMS}$, with an energy/measurement of 270nJ for the readout circuit and 2.6μJ for the scanning-circuit drivers. The energy/bit of the transceiver at 2Mb/s (with $BER < 10^{-5}$) is shown versus communication distance (Tx/Rx: 12.8/3.3pJ @7.5m), with the DCO codes given in parentheses.

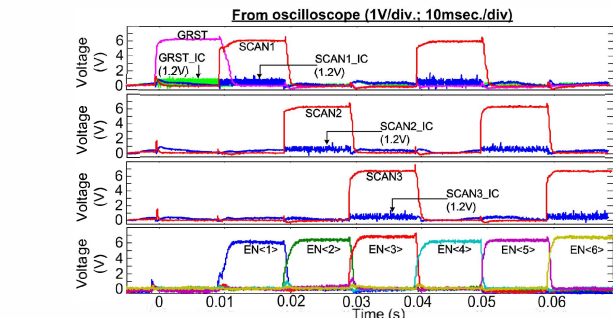


Fig. 6. Measured waveforms (oscilloscope capture), showing LAE access-circuit outputs from AC-modulated IC control signals.

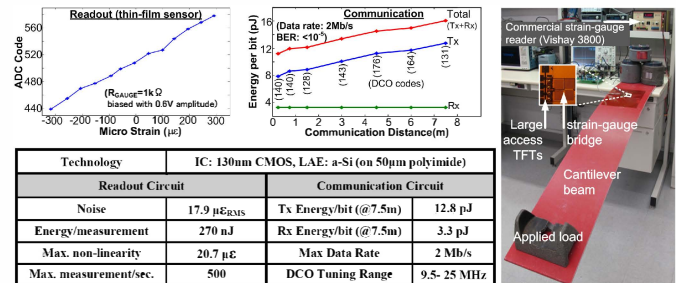


Fig. 7. Measurement summary; system tests were also performed by applying the prototype to a cantilever beam.

References

- [1] T. Someya, et al., "Organic Semiconductor Devices with Enhanced Field and Environmental Responses for Novel Applications," *MRS Bulletin*, Jul. 2008.
- [2] S. Wagner, et al., "Electronic skin: Architecture and Components," *Physica E*, Nov. 2004.
- [3] B. Hekmatshoar, et al. "Highly Stable Amorphous-Silicon Thin-Film Transistors on Clear Plastic," *Appl. Phys. Lett.*, Jul. 2008.
- [4] K. Myny, et al., "An Inductively-Coupled 64b Organic RFID Tag Operating at 13.56MHz with Data Rate of 787b/s," *ISSCC*, Feb. 2008.
- [5] L. Liu, et al., "A 107pJ/b 100kb/s 0.18m Capacitive-Coupling Transceiver for Printable Communication Sheet," *ISSCC*, Feb. 2008.